Chapter 6
Application of Chaotic Synchronization to Secure Communications

In chapters 3, 4 and 5 the phenomenon of chaotic synchronization has been studied. In this chapter, a popular application of chaotic synchronization in the area of secure communications is presented. Several chaotic communication systems with the receiver based on the chaotic synchronization concept are described. It is shown how a general approach to synchronization of chaotic flows via Lyapunov's direct method and chaotic maps via the theorems of chapter 4 can be used for the development of chaotic communication systems. The communication schemes examined include those of chaotic masking, chaotic modulation and the newly developed chaotic communication scheme of initial condition modulation. Finally, the noise performance of the chaotic parameter modulation and the initial condition modulation are compared in terms of the bit error rate. It is shown that the newly developed initial condition modulation scheme outperforms the chaotic parameter modulation scheme.

Since the onset of chaotic synchronization research, a number of demodulation techniques based on chaotic synchronization have been proposed for potential communication systems [1-13]. Of those, the following are based on the Pecora-Carroll synchronization method [1,2,4-6,8-11,13].

Pecora and Carroll's (PC) original paper on chaotic synchronization [14], suggested the application of chaotic synchronization in communications, and shortly after Oppenheim et al. presented a communication system based on the PC synchronization method [4]. The method of [4], termed "chaotic masking", was experimentally demonstrated in [5] using Chua's circuit. In this method, the information signal is added onto the chaotic carrier directly, and transmitted. The requirement of this method is that the power of the information signal has to be significantly lower than the power of the chaotic carrier [4]. In contrast to chaotic masking, a technique of "chaotic modulation" incorporates the message into the dynamical equations producing the chaotic carrier. Chaotic parameter modulation is an example of the chaotic modulation technique where a binary message modulates one or more of the system's parameters [8,9]. Other forms of chaotic modulation involve techniques where one or more of the state variables is modulated by the message [2,11,13]. As opposed to chaotic modulation, the technique of "initial condition modulation" introduces the binary message into the system through its initial conditions [10,15,16].

B. Jovic: Synchronization Techniques for Chaotic Commun. Syst., SCT 5, pp. 135–169.
springerlink.com

Communication methods based on chaotic synchronization other than PC synchronization have also been proposed. For instance in [7] chaotic masking and Pyragas' synchronization method have been used to transmit and receive information, whereas in [3] chaotic modulation and John and Amritkar (JA) synchronization method have been used.

Section 6.1 presents the communication technique of chaotic masking. The communication techniques based on chaotic modulation are presented in section 6.2. In addition, it is shown how a general approach to chaotic synchronization of flows via Lyapunov's direct method and chaotic synchronization of maps via the theorems of chapter 4 can be used in the design of chaotic communication systems. In section 6.3, a recently developed technique of initial condition modulation is presented. Finally, section 6.4 evaluates and compares the noise performance of the presented systems in terms of the bit error rate. It is shown that the initial condition modulation technique exhibits better noise performance than the chaotic parameter modulation technique.

6.1 Chaotic Masking

Chaotic masking (CM) was one of the earliest chaotic communication techniques proposed [4,5,8]. It is based on the principles of PC synchronization. It primarily involves the transmission of analog signals [4].

6.1.1 Principles of Chaotic Masking

Chaotic masking involves the addition of a message signal m to a chaotic carrier signal x, before the transmission of the sum of the two signals takes place [4]. The block diagram illustrating the principles of chaotic masking is shown in Figure 6.1 [16].

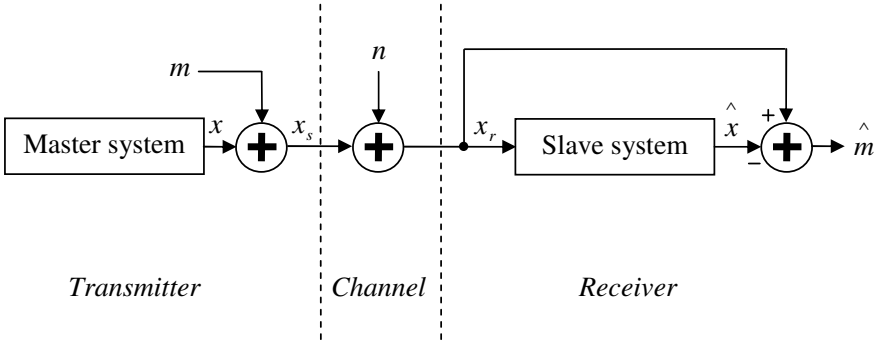

Fig. 6.1 General block diagram of the chaotic communication system based on the chaotic masking concept

In Figure 6.1 n denotes the additive white Gaussian noise (AWGN) component introduced by the channel and x_r denotes the received signal affected by AWGN. The slave system of the receiver generates a signal $\hat{x}$ which is expected to be synchronized with the corresponding master signal x of the transmitter. Assuming that the AWGN component is near zero, and that sufficient amount of time has passed for x and $\hat{x}$ to synchronize, the transmitted message m can be recovered in the form of $\hat{m}$:

$$\hat{m} = x_r - \hat{x} = (m + x) - \hat{x} \approx m \tag{6.1.1}$$

The requirement of a chaotic masking scheme is for the power of the information signal to be significantly lower than the power of the chaotic carrier.

6.1.2 Chaotic Masking within the Lorenz Master-Slave System

Chaotic masking within the Lorenz master-slave system has been demonstrated in [4,8, 9]. The system has been designed using the Lorenz x signal as the driving signal. Lyapunov's direct method has been used in [8] to show that using the x signal as the driving signal the master-slave system synchronizes. It has then also been shown that by adding a small amplitude speech signal onto the chaotic carrier one is able to recover the speech signal at the receiver. The communication system based on chaotic masking, while implementing the Lorenz master-slave system, is shown in Figure 6.2. An ability to recover the transmitted information is demonstrated under noiseless conditions in Figure 6.3 by processing the word "Oak" through the system. By comparing the top and the bottom graphs of Figure 6.3 one can see that the transmitted original message has been recovered with

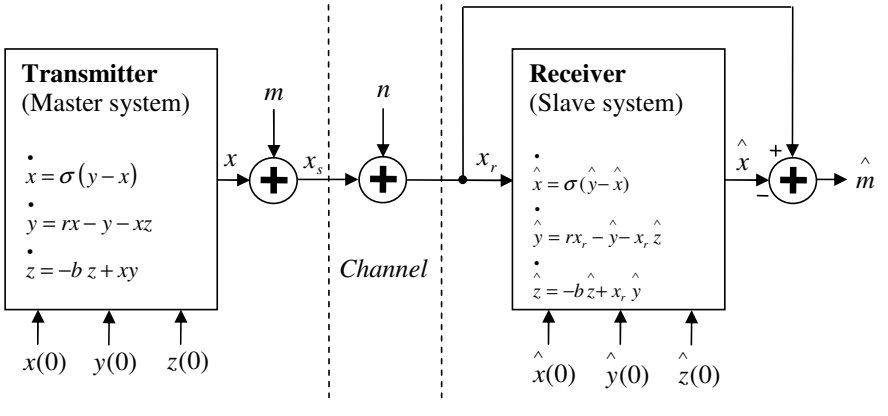

Fig. 6.2 The Lorenz based communication system implementing chaotic masking

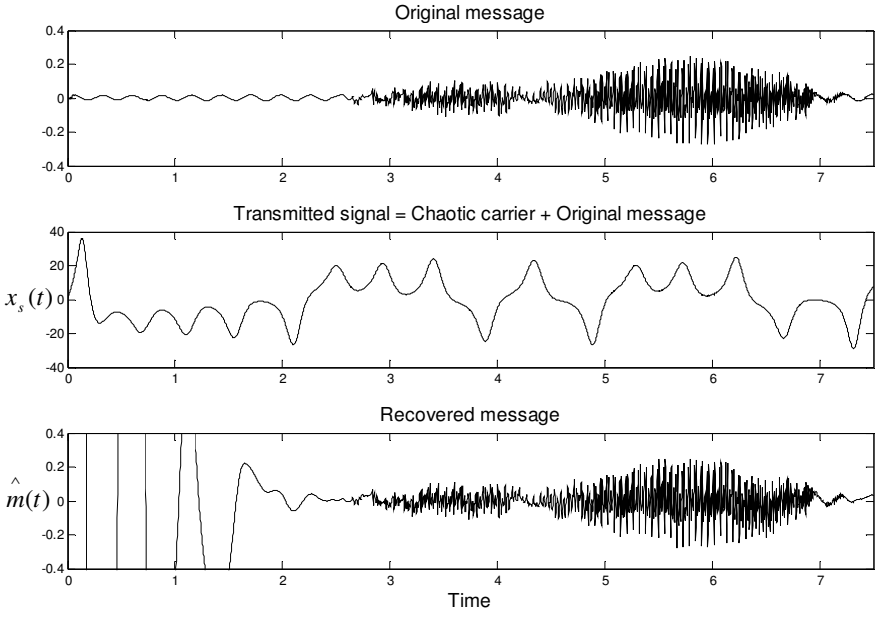

Fig. 6.3 The signals of the Lorenz based communication system implementing chaotic masking

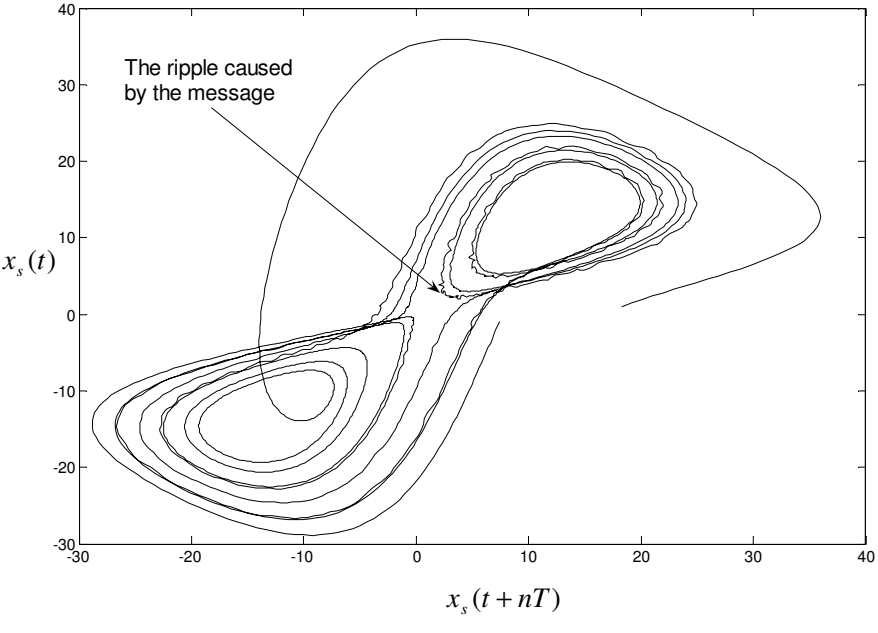

Fig. 6.4 The transmitted signal $x_s(t)$ plotted in phase space

reasonable accuracy. In the case of Figure 6.3 the chaotic parameter values of the system of Figure 6.2 have been set to: $\sigma = 16$, $r = 45.6$ and $b = 4$. An evident difference in power between the chaotic carrier and the speech signal can be observed in Figure 6.3. The transmitted signal of Figure 6.3 has been plotted in phase space in Figure 6.4. The small ripple, observed on the strange attractor of Figure 6.4, is caused by the message *m* embedded within it.

6.2 Chaotic Modulation

In the chaotic masking scheme, described above, information is added directly onto the chaotic carrier without the influence of the message on the dynamical equations producing the carrier. In contrast to chaotic masking, chaotic modulation incorporates the message into the dynamical equations producing the chaotic carrier.

6.2.1 Chaotic Parameter Modulation

As opposed to chaotic masking which is primarily used for analog transmission, chaotic parameter modulation (CPM) is used for transmission of binary information.

6.2.1.1 Principles of Chaotic Parameter Modulation

A block diagram of a chaotic communication system based on the CPM concept is shown in Figure 6.5 [16]. As for the CM scheme, a requirement for the CPM scheme is for the master-slave system to synchronize for a given driving signal, as outlined in sections 3.1-3.3.

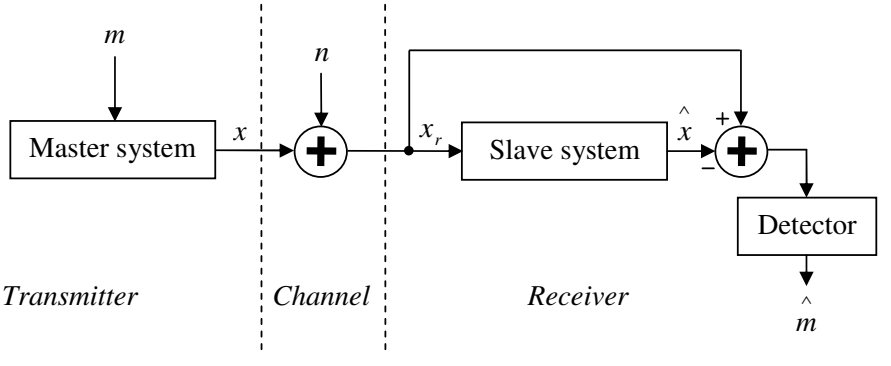

Fig. 6.5 A block diagram of the chaotic communication system based on the parameter modulation concept

In Figure 6.5, the message m varies between the two particular values, depending on whether a binary 0 or a binary 1 is to be transmitted. The message is incorporated into a certain modulating parameter of the master system causing it to change its value with the change in the message. The parameters of the slave system are fixed at all time. When the master-slave parameters are identical synchronization occurs. This forces the synchronization error to zero, indicating that bit 0 has been transmitted. Alternatively, with the master-slave parameter mismatch the system does not synchronize, indicating that bit 1 has been transmitted. Therefore, this is a form of on-off keying. This concept is illustrated in Figure 6.6. The choice of the modulating parameter of the master chaotic system must be chosen with care to ensure the chaotic properties of the system at all time. This ensures the increased security within the communication system.

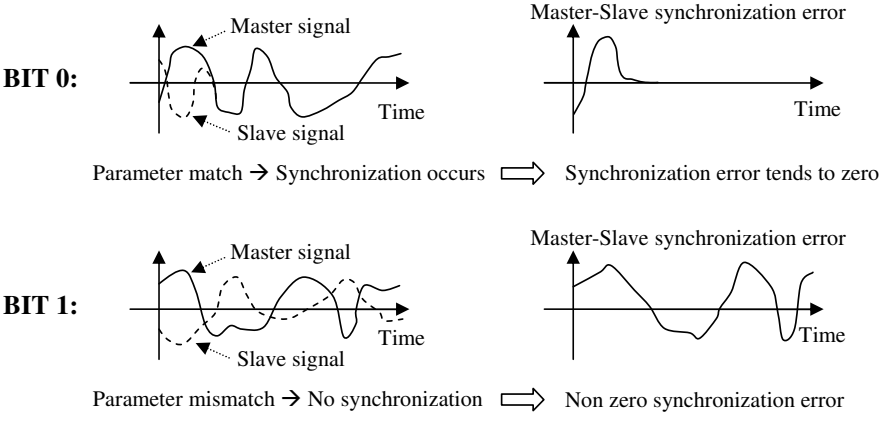

Fig. 6.6 The chaotic parameter modulation concept

6.2.1.2 Chaotic Parameter Modulation within the Lorenz Master-Slave System

The concept of parameter modulation is now demonstrated on the Lorenz master-slave chaotic system [8,9]. In [8] the binary message is used to alter the parameter b of the master (transmitter) Lorenz chaotic system between 4 and 4.4 depending on whether a bit 0 or bit 1 is to be transmitted. However, at the slave (receiver) side the parameter b is fixed at 4 for all time. Thus, the synchronization either occurs or does not, depending on the state of the parameter b at the transmitter (master) side. The parameters σ and r are fixed at 16 and 45.6, respectively. For these parameter values the system is chaotic. In order to implement the CPM scheme the authors of [8] have scaled the Lorenz chaotic system to allow for the limited dynamic range of the operational amplifiers. This system, based on the PC synchronization concept, is presented in Figure 6.7.

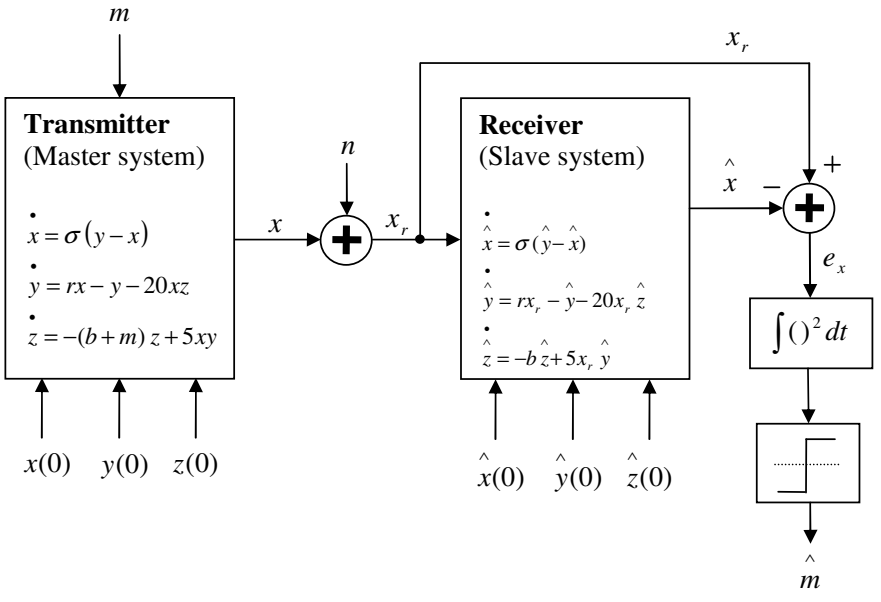

Fig. 6.7 The Lorenz based communication system implementing chaotic parameter modulation. The parameter values: $\sigma = 16$, $r = 45.6$ and $b = 4$.

The transmitted signal x, of Figure 6.7, is shown in Figure 6.8 when the series of 10 bits is transmitted, that is, when m = [0, 0, 0.4, 0, 0.4, 0.4, 0, 0.4, 0, 0.4], or in binary terms: *message* = [0 0 1 0 1 1 0 1 0 1]. Figure 6.8 also shows the corresponding squared synchronization error, e_x^2, under noiseless conditions. The received bits are detected by squaring and integrating the error e_x. The output of the integrator is then compared to the predetermined threshold and the decision is made whether a bit 0 or a bit 1 was sent. The behaviour of the system, corresponding to the master-slave parameter match (bit 0) and mismatch (bit 1), can also be illustrated in phase space. In Figure 6.9 the strange attractors corresponding to the third, fourth, fifth and sixth transmitted bit have been plotted. It can be observed from Figure 6.9 that in the case of the third, fifth and sixth bit the master-slave trajectories do not synchronize, but follow their own separate paths [16]. This is as expected due to the master-slave parameter mismatch. However, in the case of the fourth bit, the master-slave parameters match, causing the trajectories to synchronize. Note that the spreading factor of 400 has been used to represent one bit. By definition the spreading factor denotes the number of discrete sample points (chips) contained within one information bit. It is the ratio of a bit period to a chip period [17]. A spreading factor that is too small may be insufficient for synchronization to take place and thus make it more difficult to decode the transmitted information. Alternatively, a spreading factor that is too large may be impractical from the bandwidth point of view. A transient period of 1000 chips has been

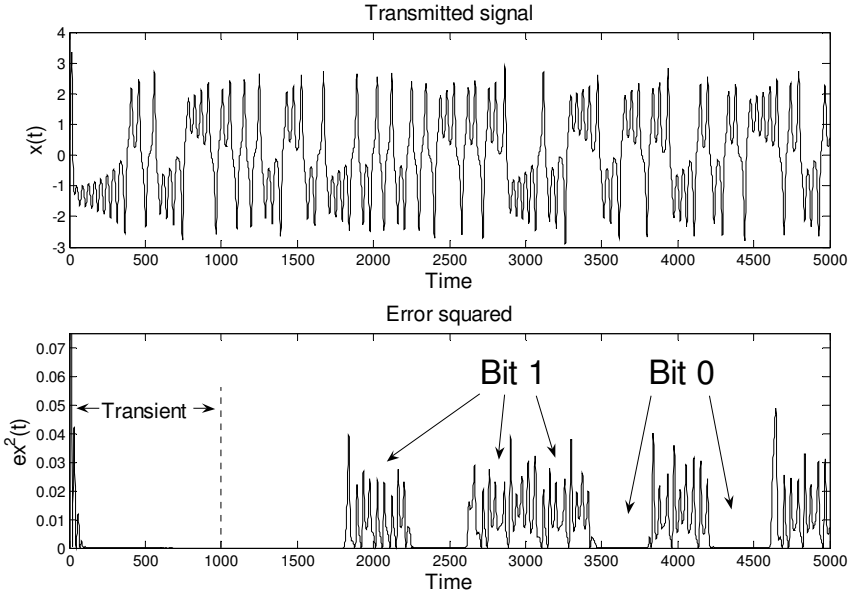

Fig. 6.8 The transmitted signal x and the squared synchronization error e_x^2

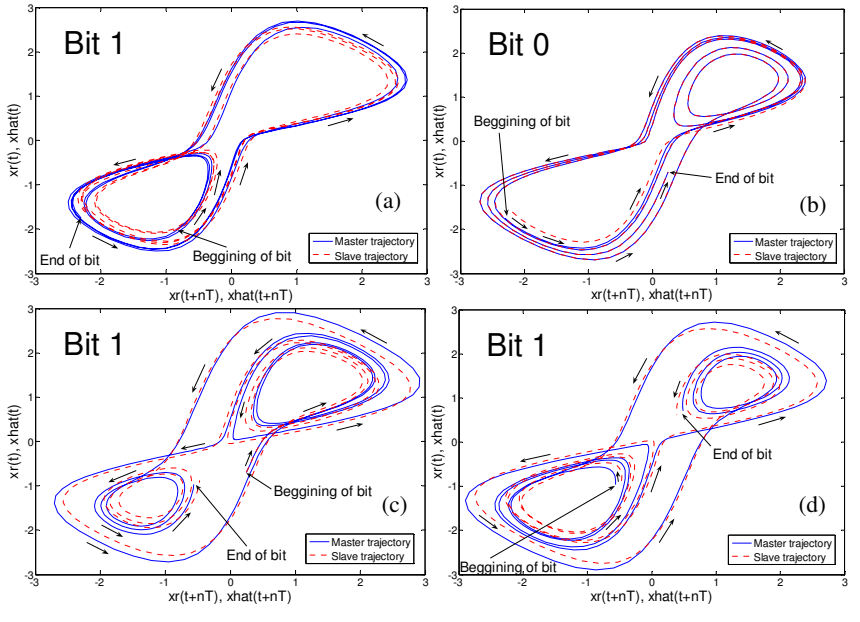

Fig. 6.9 Phase space representation of the received signal x_r and the corresponding slave signal $\hat{x}$ for: (a) the 3rd bit of the transmitted message sequence: [0 0 1 0 1 1 0 1 0 1], (b) the 4th bit, (c) the 5th bit, and (d) the 6th bit.

allowed for the case of Figure 6.8. During the transient period there is no data transmission taking place.

6.2.2 General Approach to Chaotic Parameter Modulation

In this subsection, a general approach to chaotic parameter modulation is developed. It involves the design of the nonlinear controller via Lyapunov's direct method, as outlined in section 3.3. In contrast to the CPM scheme presented in subsection 6.2.1, the scheme presented here does not rely on the inherent synchronization properties of the master-slave system for a given drive signal. It instead enforces synchronization upon the master-slave system by designing the control laws which ensure asymptotic stability within the system.

6.2.2.1 Principles of the General Approach to Chaotic Parameter Modulation

Consider a general block diagram, given in Figure 6.10 [16], of the chaotic communication system based on the parameter modulation concept.

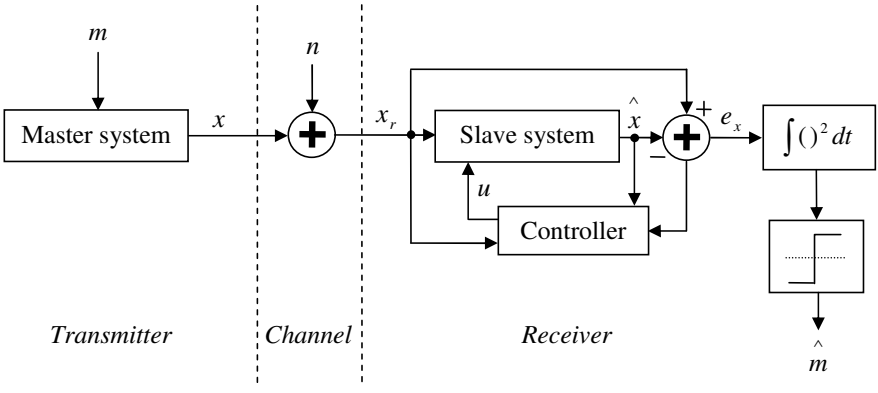

Fig. 6.10 General block diagram of the chaotic communication system based on the parameter modulation concept

In Figure 6.10, the binary message m is introduced into the system by varying one or more of the parameters of the master system. As in subsection 6.2.1, the parameters of the slave system are fixed at all time. Therefore, synchronization occurs or not, depending on the state of the parameters at the transmitter side. The controller of Figure 6.10 is designed via Lyapunov's direct method, as outlined in section 3.3. The controller output, u, then ensures the synchronization of the master-slave system when the master-slave parameters match. Note that, in general, the signal x may be an interleaved version of more than one signal of the master system [10], such as in a TDM system, as discussed in chapters 8 and 9.

6.2.2.2 Chaotic Parameter Modulation within the Ueda Master-Slave System

Here the control law for the Ueda master-slave chaotic system, with the master signal x driving, is designed. The system is then applied to a CPM based communication system. In order to justify a design of a controller for the Ueda master-slave chaotic system its inherent synchronization properties without the controller must first be investigated. Figure 6.11, shows the Ueda master-slave chaotic system with the master signal x driving. The dynamics of the Ueda master chaotic system are shown in Figure 6.12. In Figure 6.11, the initial conditions of the master-slave z signals have been set to an equal value. As will be shown, with the initial conditions so chosen the controller design is significantly simplified. In Figure 6.13, the synchronization errors for the x, y and z master-slave chaotic signals are shown. These errors demonstrate that the master-slave x signals of the system of Figure 6.11 do not synchronize and thus the system warrants a controller design. Note that the master-slave system synchronization error has been defined by equation 6.2.1:

$$e_1(t) = x(t) - \hat{x}(t), \qquad e_2(t) = y(t) - \hat{y}(t), \qquad e_3(t) = z(t) - \hat{z}(t). \tag{6.2.1}$$

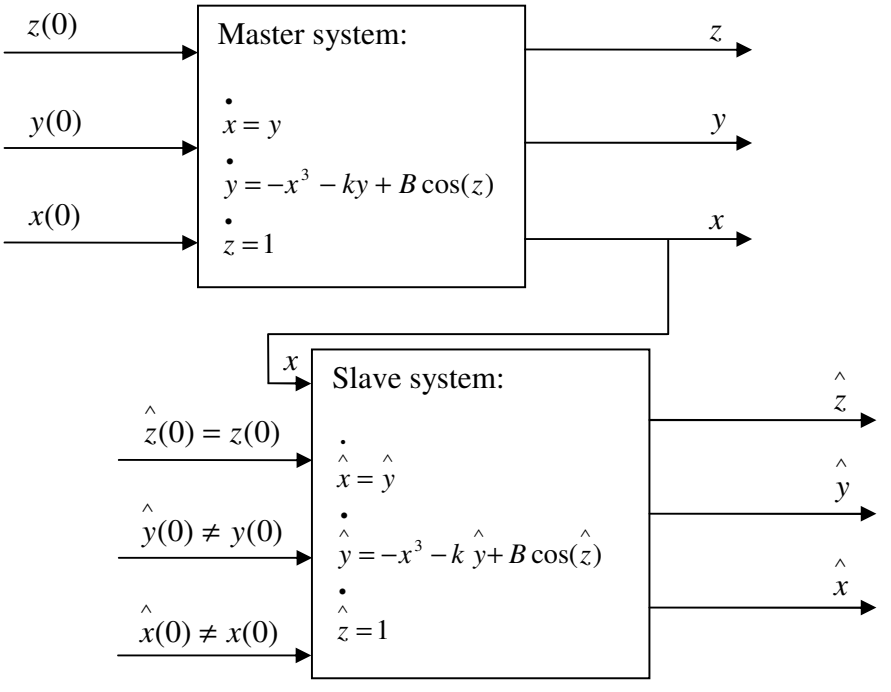

Fig. 6.11 The block diagram of the Ueda master-slave chaotic system, with the x signal driving. The parameter values are $k = 0.05$, $B = 7.5$. Note that this system differs from that of Figure 5.9 of chapter 5 in that $\hat{x} \neq x$.

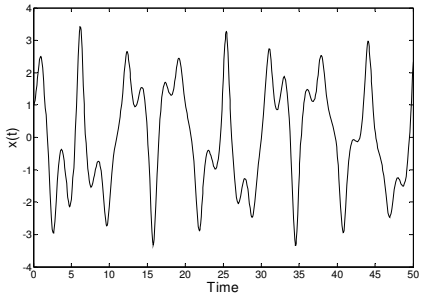

Fig. 6.12a The Ueda chaotic time series, $x(t)$

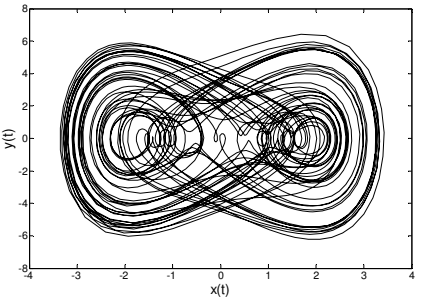

Fig. 6.12b The Ueda strange attractor

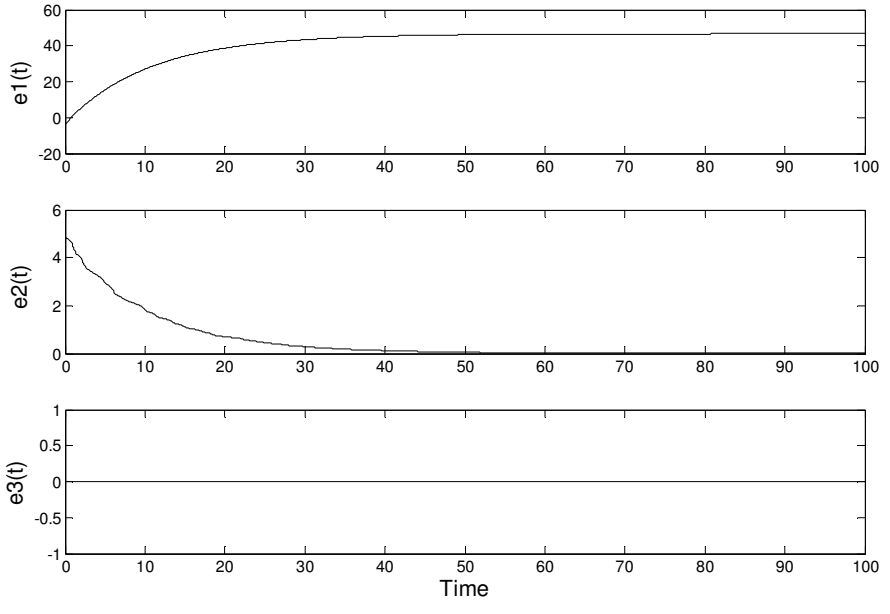

Fig. 6.13 Inherent synchronization error of the Ueda master-slave chaotic signals without the controller

Consider the CPM Ueda communication system of Figure 6.14. The constants f and g of the master system can be of any value and are chosen so that the parameters k and B take on the appropriate values for a given m.

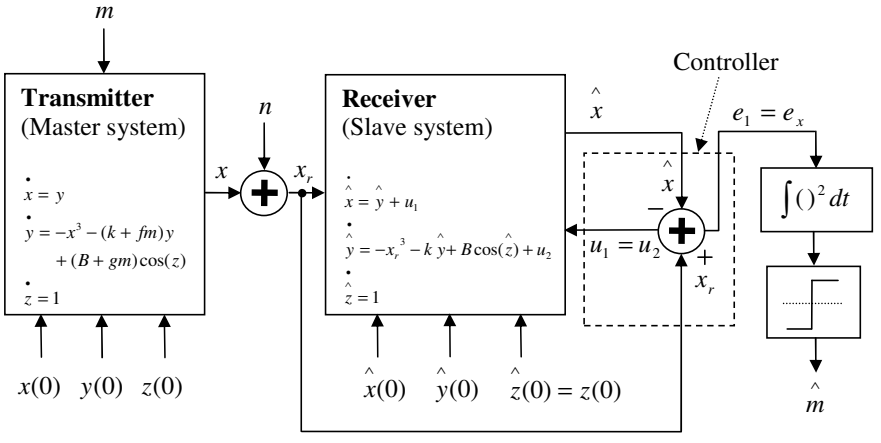

Fig. 6.14 The Ueda chaotic communication system based on the parameter modulation concept

In order to demonstrate the design of the controller of Figure 6.14 assume no noise in the system. It follows then that: $x_r = x$, so that the slave system, including the control laws, takes the form given by equation 6.2.2:

$$\begin{aligned} \dot{\hat{x}} &= \hat{y} + u_1 \\ \dot{\hat{y}} &= -x^3 - k\hat{y} + B\cos(\hat{z}) + u_2 \\ \dot{\hat{z}} &= 1 \end{aligned} \tag{6.2.2}$$

The differential synchronization error of the master-slave system of Figure 6.14 is then given by equation 6.2.3:

$$\begin{aligned} \dot{e}_1 &= \dot{x} - \dot{\hat{x}} = y - \hat{y} - u_1 \\ \dot{e}_2 &= \dot{y} - \dot{\hat{y}} = -ky + k\hat{y} + B\cos(z) - B\cos(\hat{z}) - u_2 \\ \dot{e}_3 &= \dot{z} - \dot{\hat{z}} = 0 \end{aligned} \tag{6.2.3}$$

The difference between the master-slave z signals is governed by equation 6.2.6 [10]:

$$\dot{z} = \dot{\hat{z}} \tag{6.2.4}$$

$$\int \dot{z}\, dt = \int \dot{\hat{z}}\, dt \tag{6.2.5}$$

$$z - \hat{z} = z(0) - \hat{z}(0) \tag{6.2.6}$$

Given that the master-slave z initial conditions are equal to each other, or that their difference is equal to $\pm 2n\pi$, where n is any integer, equation 6.2.6 can be reduced to equation 6.2.7 [10]:

$$z - \hat{z} = \pm 2n\pi \tag{6.2.7}$$

Using the standard trigonometric identities, equation 6.2.3 can be rewritten in the form of equation 6.2.8:

$$\begin{aligned}
\dot{e}_1 &= \dot{x} - \dot{\hat{x}} = y - \hat{y} - u_1 \\
\dot{e}_2 &= \dot{y} - \dot{\hat{y}} = -ky + k\hat{y} + 2B \sin\left(\frac{z+\hat{z}}{2}\right) \sin\left(\frac{z-\hat{z}}{2}\right) - u_2 \\
\dot{e}_3 &= \dot{z} - \dot{\hat{z}} = 0
\end{aligned} \tag{6.2.8}$$

Substituting equation 6.2.7 into equation 6.2.8, equation 6.2.9 is obtained:

$$\begin{aligned}
\dot{e}_1 &= \dot{x} - \dot{\hat{x}} = y - \hat{y} - u_1 \\
\dot{e}_2 &= \dot{y} - \dot{\hat{y}} = -ky + k\hat{y} + 2B \sin\left(\frac{z+\hat{z}}{2}\right) \sin(\pm n\pi) - u_2 \\
\dot{e}_3 &= \dot{z} - \dot{\hat{z}} = 0
\end{aligned} \tag{6.2.9}$$

Finally simplifying equation 6.2.9, equation 6.2.10 is obtained:

$$\begin{aligned} \dot{e}_1 &= e_2 - u_1 \\ \dot{e}_2 &= -ke_2 - u_2 \\ \dot{e}_3 &= 0 \end{aligned} \tag{6.2.10}$$

In order to design the controller for this particular master-slave system, consider the candidate Lyapunov function given by equation 6.2.11:

$$V = \frac{1}{2}(e_1^2 + e_2^2) \tag{6.2.11}$$

Differentiating equation 6.2.11 with respect to time equation 6.2.12 is obtained:

$$\dot{V} = \dot{e}_1 e_1 + \dot{e}_2 e_2 \tag{6.2.12}$$

Substituting equation 6.2.10 into equation 6.2.12 and simplifying, equation 6.2.13 is obtained:

$$\dot{V} = e_1 e_2 - e_1 u_1 - ke_2^2 - e_2 u_2 \tag{6.2.13}$$

For equation 6.2.11 to be the Lyapunov function, equation 6.2.13 must be negative semi-definite. In order for equation 6.2.13 to become negative semi-definite the term $e_1 e_2$ must be eliminated, while the term $-e_1^2$ must be introduced. It is readily verifiable that this is achieved with the control laws of equations 6.2.15 and 6.2.17:

$$-e_1 u_1 = -e_1^2 \tag{6.2.14}$$

$$u_1 = e_1 \tag{6.2.15}$$

$$-e_2 u_2 + e_1 e_2 = 0 \tag{6.2.16}$$

$$u_2 = e_1 \tag{6.2.17}$$

From equations 6.2.15 and 6.2.17 it can be seen that the control laws are identical, as shown in Figure 6.14. The functionality of the control laws of equations 6.2.15 and 6.2.17 is demonstrated in Figure 6.15 from which it can be observed that all of the master-slave signals synchronize.

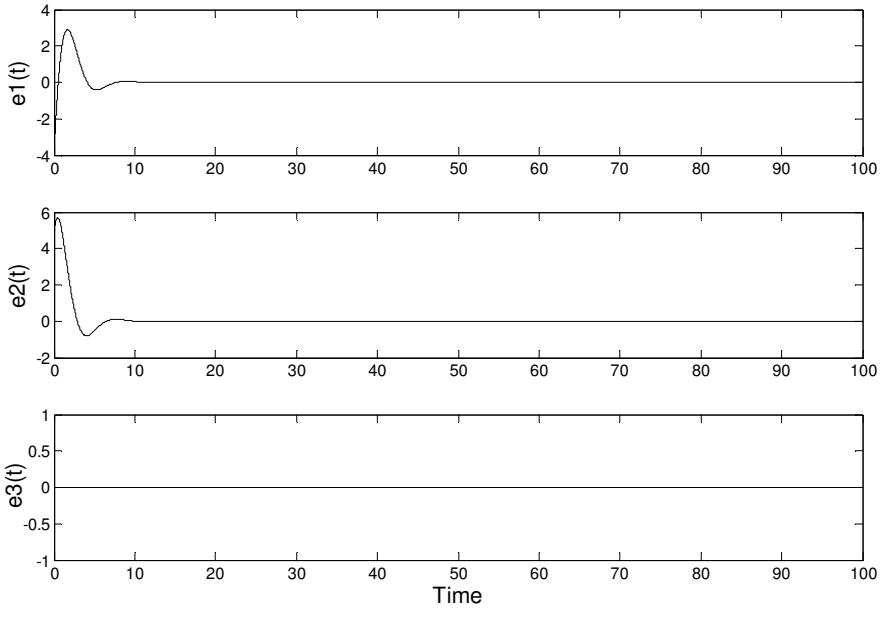

Fig. 6.15 Synchronization error of the Ueda master-slave chaotic signals with the controller

In Figure 6.14 the master system parameter set of $k = 0.05$ and $B = 7.5$ has been chosen to represent a bit 0. The master system parameter set of $k = 0.1$ and $B = 10$ has been chosen to represent a bit 1. Thus, the constants f and g of the master system of Figure 6.14 are set at 0.05 and 2.5, respectively. This allows for the adjustment of parameters k and B when bit 1 is to be transmitted. The slave system parameters are set for all time at $k = 0.05$ and $B = 7.5$, so that synchronization at the receiver side signals a bit 0 and de-synchronization signals a bit 1. Both parameter sets, $k = 0.05$, $B = 7.5$ and $k = 0.1$, $B = 10$ generate chaotic behaviour within the system [18].

The transmitted signal x is shown in Figure 6.16 when the series of 10 bits is transmitted, that is, when m = [0 0 1 0 1 1 0 1 0 1]. Figure 6.16 also shows the corresponding squared synchronization error, e_x^2, under noiseless conditions. As for the Lorenz based CPM scheme, the spreading factor of 400 has been used.

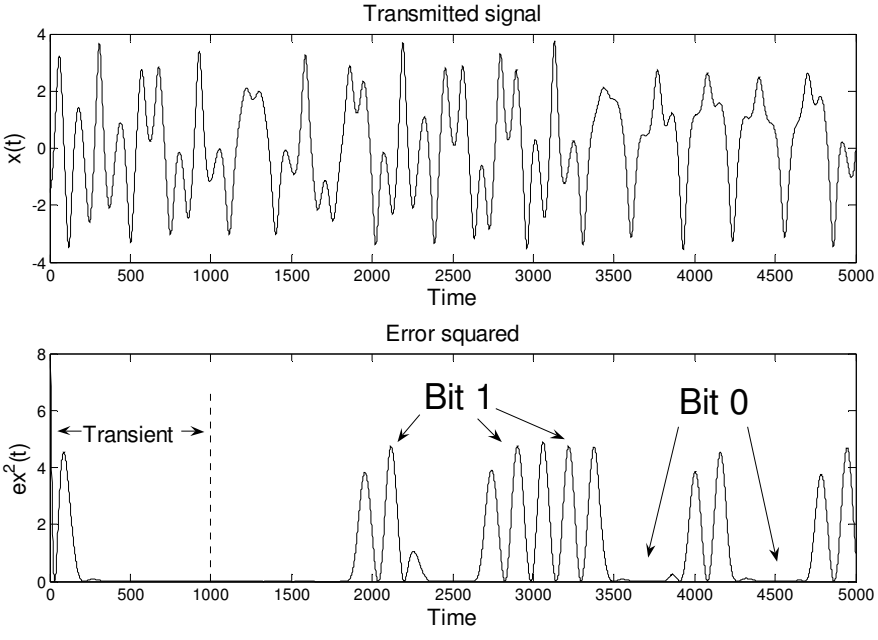

Fig. 6.16 The transmitted signal x and the squared synchronization error e_x^2

6.2.2.3 Chaotic Parameter Modulation within the Cubic Map Master-Slave System

The method of implementing the synchronized chaotic map master-slave system of chapter 4 within a CPM based communication system is now demonstrated on the $\Re^1$ cubic map. It is thus shown that one can apply either a flow or a map to a CPM based communication system when the nonlinear control laws are designed in such a way to cause synchronization among the master and slave systems. Furthermore, it is shown that the instant synchronization, as defined in chapter 4, within CPM based communication systems is of particular importance. In chapter 10, the CPM based communication system is demonstrated on the $\Re^2$ Burgers' chaotic map and its security evaluated and compared to the other chaotic communication systems.

The CPM based chaotic communication system implementing the cubic map master-slave system and the nonlinear controller of Figure 4.3, section 4.2, is shown in Figure 6.17.

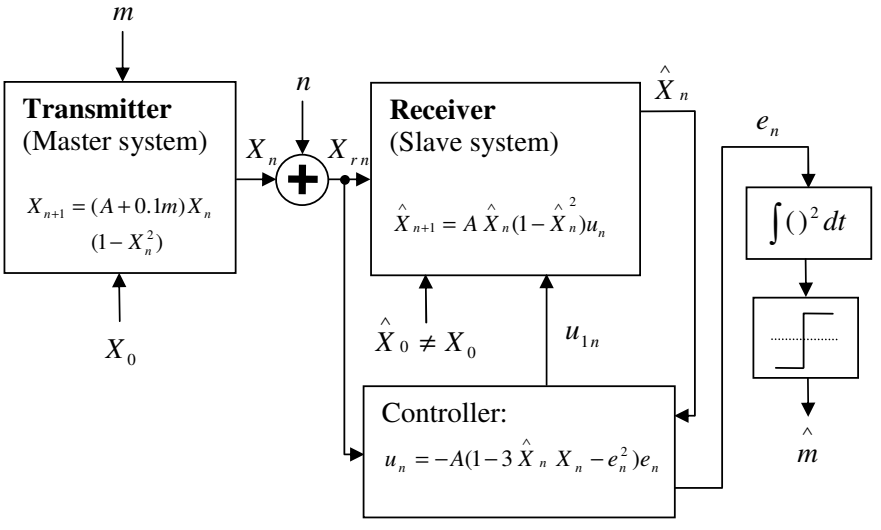

Fig. 6.17 The cubic map chaotic communication system based on the parameter modulation concept

In Figure 6.17, the master system parameter $A = 2.9$ has been chosen to represent a bit 0. The master system parameter $A = 3$ has been chosen to represent a bit 1. The message *m* of Figure 6.17 takes on the values of 0 and 1 depending on the polarity of a bit transmitted. The slave system parameter *A* is set for all time at $A = 2.9$, so that synchronization at the receiver side signals a bit 0 and desynchronization signals a bit 1. Both parameter values, $A = 2.9$ and $A = 3$, generate chaotic behaviour within the system.

The transmitted signal X_n is shown in Figure 6.18 when the series of 10 bits is transmitted, that is, when *m* = [0 0 1 0 1 1 0 1 0 1]. Figure 6.18, also shows the corresponding squared synchronization error, e_n^2, under noiseless conditions, that is, when *n* = 0. The squared synchronization error, e_n^2, is shown for the three different cases, that is, when the eigenvalues are equal to 1, 0.99 and 0. As for the Lorenz and Ueda CPM based schemes, the spreading factor of 400 has been used. A transient period of 10 chips has been allowed for the case of Figure 6.18.

It can be observed from Figure 6.18c that the system exhibits the worst performance when the eigenvalue of the system is equal to 1. This is to be expected as when the eigenvalue is outside the unit circle in the *z* domain the system does not synchronize even when the master-slave parameters match. Thus, in this case, the receiver cannot discriminate among bits 0 and 1. In contrast to this, it can be observed from Figure 6.18d that when the eigenvalue is just within the unit circle, that is, at 0.99, the system synchronizes for bits 0 and does not for bits 1. However, as can be seen from Figure 6.18d, the time it takes to synchronize is long and thus affects the performance of the system by impeding with the time period of the

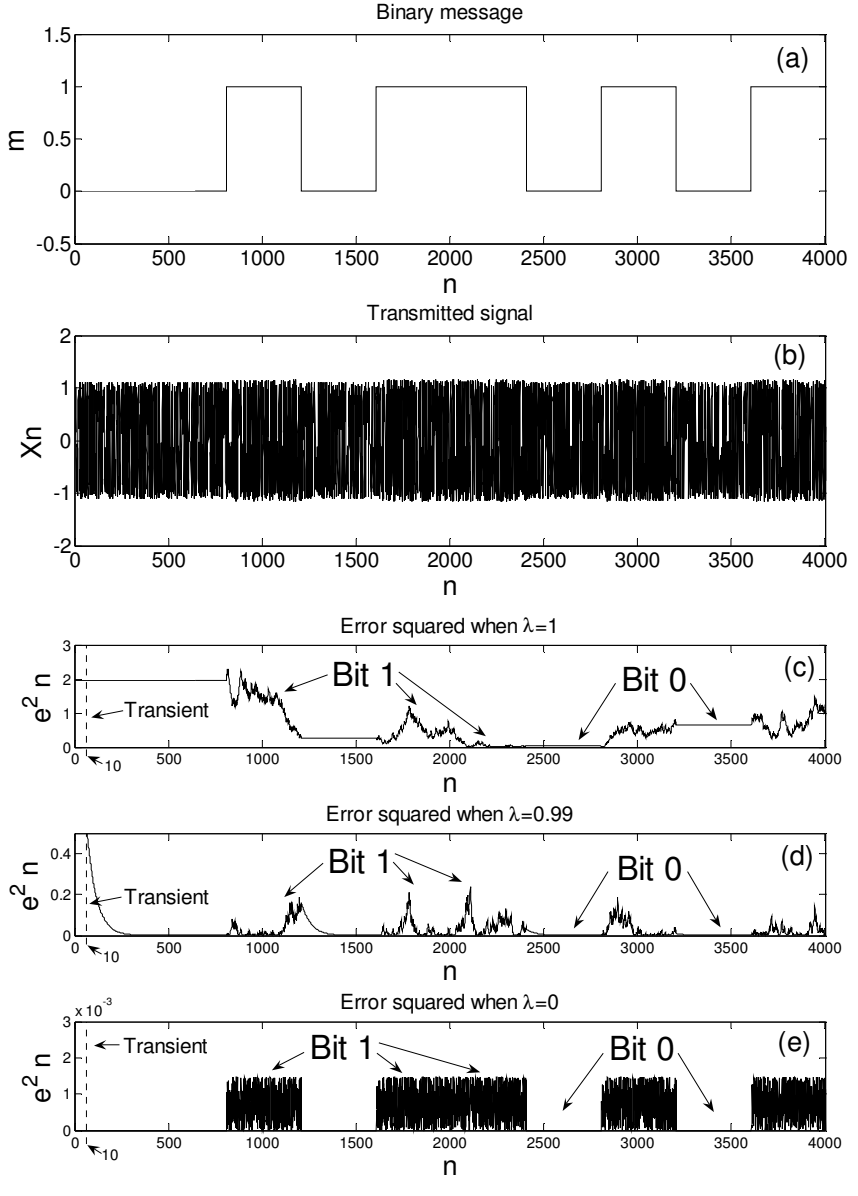

Fig. 6.18 (a) The binary message *m*, (b) The transmitted signal X_n, and: The squared synchronization error e_n^2 when: (c) $\lambda = 1$, that is, when the control law: $u_n = (1 - A(1 - 3\hat{X}_n X_n - e_n^2))e_n$, (d) $\lambda = 0.99$, that is, when the control law: $u_n = (0.99 - A(1 - 3\hat{X}_n X_n - e_n^2))e_n$, (e) $\lambda = 0$, that is, with the control law of Figure 6.17.

next bit. Finally, with the eigenvalue at 0, that is, with the error system at 0, in this $\Re_1$ case, synchronization with the matched parameters is instant. As can be seen by comparing Figures 6.18c, d and e, this allows for the most efficient discrimination among bits 0 and 1.

6.2.3 Other Forms of Chaotic Modulation

In the case of chaotic parameter modulation, the binary message is introduced into the dynamical equations of the system through one or more of the system's parameters. Alternatively, it is also possible to introduce the message into the dynamical equations of the system by incorporating it into one or more of the system's state variables. For instance, in [11,2] a binary message has been incorporated into the dynamics of the Chua master-slave system. Also, in [11], a chaotic communication system with a sinusoidal message incorporated into the dynamics of the Lorenz master-slave chaotic system has been presented. Furthermore, Lyapunov's direct method has been used to prove that the master-slave system must synchronize in the presence of the message. Using a similar approach to the one of [11,19], the authors of [13] introduce the message into the system through the x state variable. However, in this case, the message is recovered through an extra, purpose designed, state variable of the system.

The principles of operation of the Lorenz based chaotic communication system of [11], are now briefly demonstrated. The system is shown in Figure 6.19. Note that the Lorenz chaotic system has been modified here by introducing the parameter μ. The asymptotic stability within the master-slave system of Figure 6.19 has been demonstrated in [11], by showing the existence of the Lyapunov function:

$$V = \frac{1}{2}\left(\frac{1}{\sigma}e_1^2 + e_2^2 + e_3^2\right) \tag{6.2.18}$$

where: $e_1(t) = \hat{x}(t) - x(t)$, $e_2(t) = \hat{y}(t) - y(t)$, $e_3(t) = \hat{z}(t) - z(t)$.

Therefore, under noiseless conditions, the master-slave x signals must synchronize for a given drive signal $x_r = x + m$. Assuming that the sufficient amount of time has passed for x and $\hat{x}$ to synchronize, the transmitted message m can then be exactly recovered in the form of $\hat{m}$:

$$\hat{m} = x_r - \hat{x} = (x + m) - \hat{x} = m \tag{6.2.19}$$

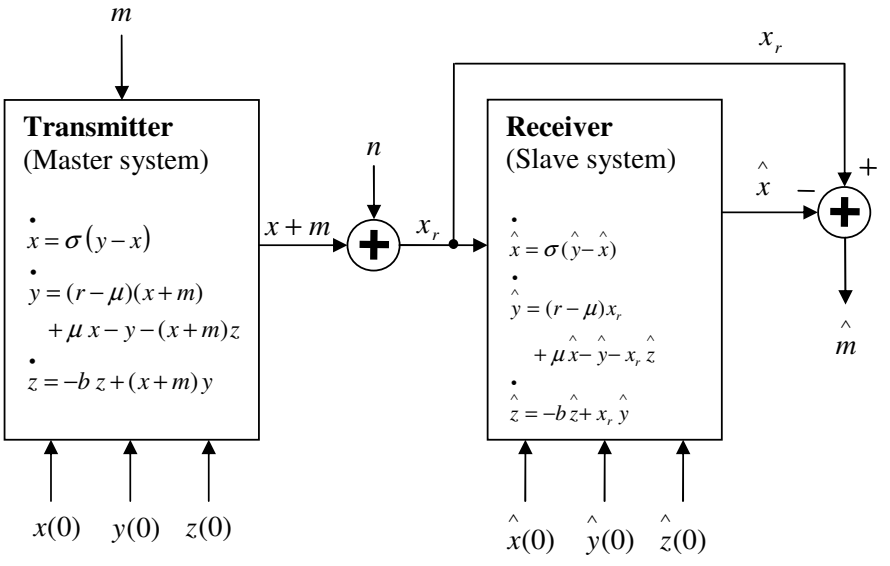

Fig. 6.19 The Lorenz based chaotic communication system of [11]. The parameter values: $\sigma = 16$, $r = 45.6$, $b = 4$ and $\mu = 0.98$.

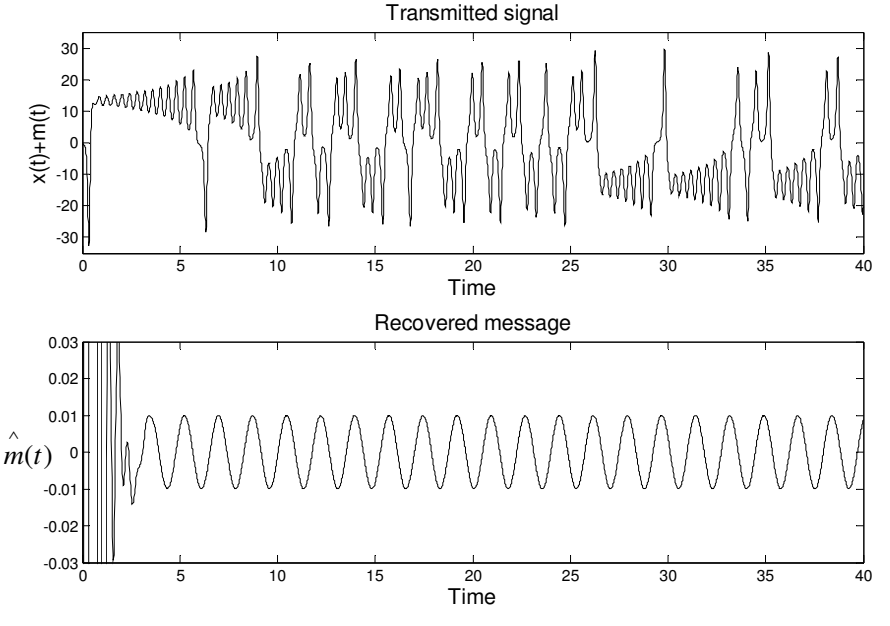

Fig. 6.20 The transmitted signal $x + m$ and the recovered message $\hat{m}$

Figure 6.20 demonstrates the operation of the system in a noiseless environment when: $m = A_m \sin(2\pi f_m)$, and: $A_m = 0.01$, $f_m = 1.8/\pi$ [11]. The upper graph of Figure 6.20 shows the transmitted signal $x + m$. From the lower graph of Figure 6.20 it can be observed that as the transients die out the sinusoidal message remains.

6.3 Initial Condition Modulation

This section presents a recently developed chaotic communication technique based on the initial condition modulation (ICM) of the chaotic carrier by the binary message, published in [10,16]. The chaotic modulation techniques of section 6.2 introduce the message into the system by incorporating it into the dynamical equations of the system. In contrast to those, the ICM technique introduces the message into the system through the system's initial conditions. The ICM technique is based on the principles of the novel mathematical analysis for predicting master-slave synchronization presented in chapter 5 [10].

6.3.1 Principles of Initial Condition Modulation

A general block diagram of a chaotic communication system based on the initial condition modulation concept is shown in Figure 6.21. The binary message *m* is introduced into the system through an initial condition (*IC*) of one of the master signals. The choice of the initial condition depends on the synchronization properties of the particular master-slave system under consideration. Using the mathematical analysis of chapter 5 [10], it is often possible to show that the mathematical expression for the synchronization error of the master-slave signals can be expressed in terms of the initial conditions of the system. The communication system is then designed by choosing two different sets of initial conditions to represent binary symbols 0 and 1. To represent a bit 0 the master-slave initial conditions are so chosen to cause the system to synchronize, that is, to cause the synchronization error to go to zero. Alternatively, to represent bit 1, the master-slave initial conditions are so chosen to inhibit synchronization. Therefore the operation of the ICM scheme resembles that of the CPM scheme in that they both rely on the state of the synchronization error at the receiver. However, the ICM scheme operates in accordance with the mathematical expression for the synchronization error. In general, the signal *x* may be an interleaved version of more than one signal of the master system [10].

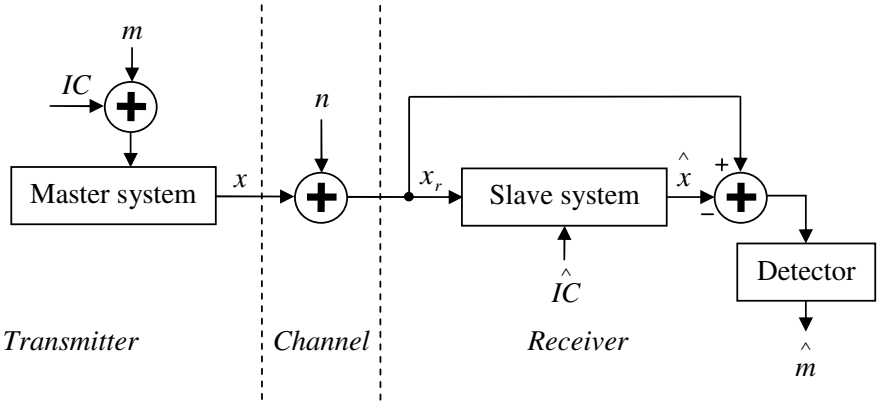

Fig. 6.21 A block diagram of the chaotic communication system based on the initial condition modulation concept

6.3.2 *Initial Condition Modulation within the Ueda Master-Slave Chaotic System*

Consider the Ueda master-slave chaotic system of Figure 5.9, section 5.3, when the master signal x drives. It has been shown in section 5.3 that in this configuration equation 5.3.19, repeated below as equation 6.3.1, governs the synchronization error of the master-slave y signals [10]:

$$y(t_o) - \hat{y}(t_o) = A - k\int_{t=0}^{t=t_o} (y(t) - \hat{y}(t))dt + 2B\sin(\phi)\sin(t_o + \Omega) \qquad (6.3.1)$$

where: $$\phi = \frac{z - \hat{z}}{2} = \frac{z(0) - \hat{z}(0)}{2}, \qquad \Omega = \phi + \hat{z}(0) + \frac{\pi}{2}.$$

In addition, it has also been shown in section 5.3 [10] that as time tends to infinity equation 6.3.1 settles to the steady state behaviour governed by its third term. Furthermore, note that the third term of equation 6.3.1 is governed by the initial conditions of the master-slave z signals. By observing equation 6.3.1 it is then readily verifiable that the error of the master-slave y signals tends to zero when the difference among the master-slave z initial conditions is equal to $\pm 2n\pi$ (where n is any integer). Alternatively, when the difference is equal to $\pm n\pi$, (where n is any odd integer), the error of the master-slave y signals reaches its maximum possible value. These two chaotic synchronization properties of the Ueda master-slave chaotic system have been utilized to construct the communication system of Figure 6.22. The master initial condition of the z signal is varied according to the value of the bit to be transmitted, bit 0 being represented by $m = 2\pi$ and bit 1 by $m = \pi$. In this way, the overall difference among the

master-slave z initial conditions entering the transmitter and the receiver is equal to either π or 2π. Therefore, under noiseless conditions, the system either synchronizes or does not [10].

As explained in chapter 1, for optimal performance of the system in the AWGN channel, it is essential that the symbols (bits) are as far apart as possible in their symbol space [20]. For the communication system of Figure 6.22 the separation of symbols 0 and 1 in their symbol space is largest when the difference among the master-slave z initial conditions is equal to $\pm 2n\pi$ (where n is any integer) and $\pm n\pi$, (where n is any odd integer), respectively. These two properties of the Ueda master-slave chaotic system are expressed by equations 5.3.25 and 5.3.28 and illustrated by Figures 5.13b and 5.14b of section 5.3.

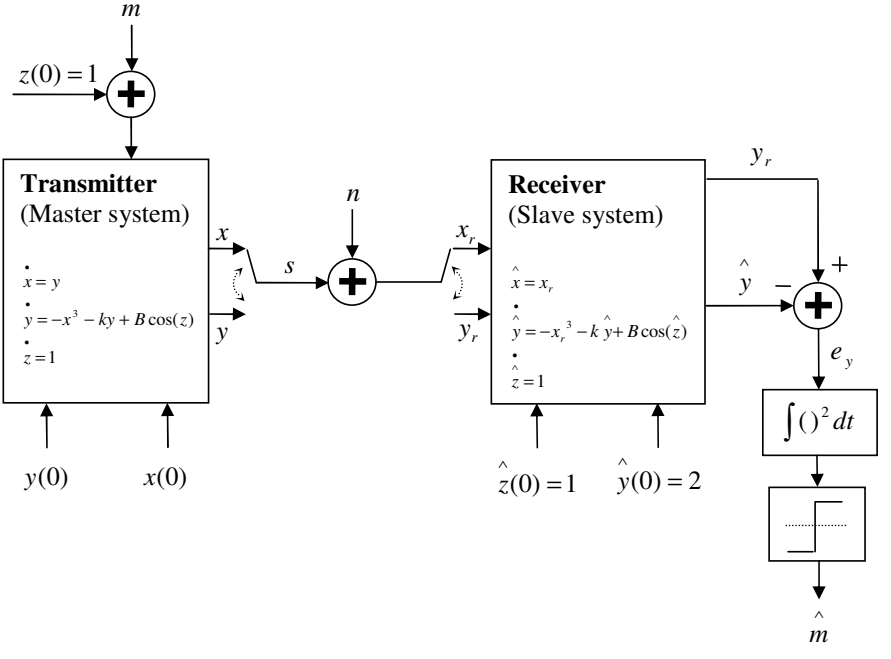

Fig. 6.22 The Ueda chaotic communication system based on the initial condition modulation

In order to evaluate e_y at the receiver, both master signals x and y, must be transmitted. Therefore, in Figure 6.22, the transmitted signal s is a signal composed of x and y master signals interleaved in the fashion described by Eqs. 6.3.2 and 6.3.3, respectively [10]:

$$x(t) = \sum_{i=1}^{N} x_t \delta(t - 2n + 1) \qquad (6.3.2) \qquad\qquad y(t) = \sum_{i=1}^{N} y_t \delta(t - 2n) \qquad (6.3.3)$$

In equations 6.3.2 and 6.3.3 $\delta(t)$ is the impulse function and N is the spreading factor, that is, the number of x (y) chaotic points representing a single bit.

The x_r and y_r signals, at the receiver side of Figure 6.22, represent the noisy x and y signals of the transmitted signal, where n denotes AWGN, composed of the two components represented in time domain by equations 6.3.4 and 6.3.5:

$$n_x(t) = \sum_{i=1}^{N} n_{x\,t}\, \delta(t - 2i + 1) \tag{6.3.4}$$

$$n_y(t) = \sum_{i=1}^{N} n_{y\,t}\, \delta(t - 2i) \tag{6.3.5}$$

The x_r and y_r signals are represented by equations 6.3.6 and 6.3.7, respectively:

$$x_r(t) = x(t) + n_x(t) = \sum_{i=1}^{N} (x_t + n_{x\,t})\, \delta(t - 2i + 1) \tag{6.3.6}$$

$$y_r(t) = y(t) + n_y(t) = \sum_{i=1}^{N} (y_t + n_{y\,t})\, \delta(t - 2i) \tag{6.3.7}$$

In order to avoid periodicity of chaotic sequences representing bit 0 (or bit 1), it is essential to alter $x(0)$ and $y(0)$ with every new bit sent. Also, in order to ensure the continuity of the smooth nature of the signals at the transition of the transmitted bits, the initial conditions of x and y for every new bit transmitted are chosen as the final values of the chaotic carrier of the preceding bit. The interleaved transmitted signal s is shown in Figure 6.23 when the series of 10 bits is transmitted, that is, when m = [2π, 2π, π, 2π, π, π, 2π, π, 2π, π], or in binary terms: *message* = [0 0 1 0 1 1 0 1 0 1]. Figure 6.23 also shows the corresponding squared synchronization error, e_y^2, under noiseless conditions. The spreading factor of 400 has been used.

In order to demonstrate the performance of the Ueda ICM based communication system of Figure 6.22, an empirical BER curve has been produced and compared to the BER curve of the BPSK communication system [20,21]. In addition, an empirical BER curve of the Lorenz based CPM scheme presented above [8] has also been produced [21]. The results of the BER analysis are displayed in Figure 6.24. From Figure 6.24 it is observed that it requires 13-14 dB less energy per bit to achieve the same probability of error using the Ueda ICM based system of Figure 6.22 as compared to the Lorenz CPM based system of [8]. The empirical BER curves have been obtained in the following manner. The bit energy was obtained by first determining the average power of the chaotic carrier and

multiplying it by the bit period [10,20]. Then for specified bit energy to noise power spectral density ratio (E_b / N_o), the required power (variance) of noise was calculated and thus white Gaussian noise of that power generated. Finally for each E_b / N_o the probability of error, that is the bit error rate, was determined.

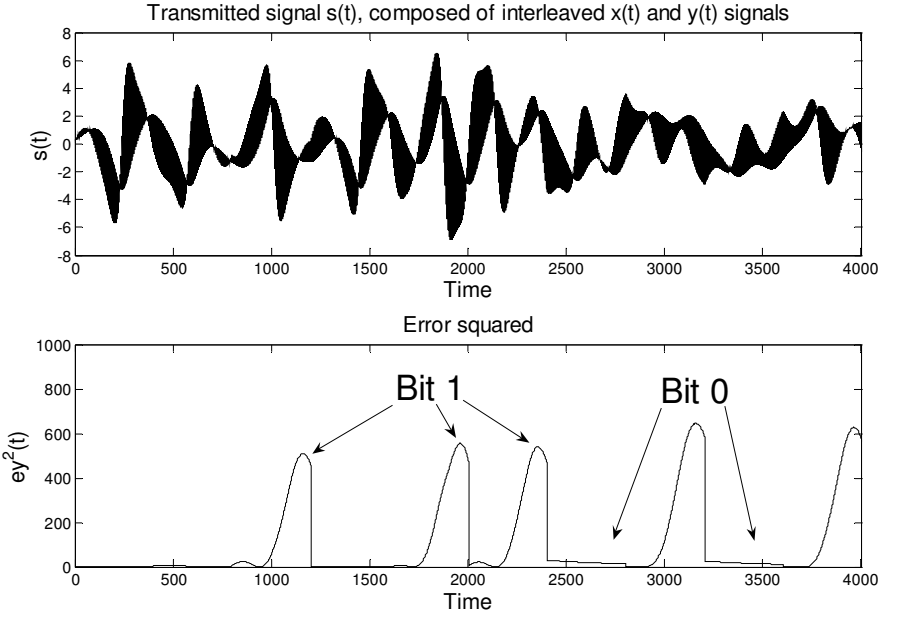

Fig. 6.23 The interleaved transmitted signal *s*, and the squared synchronization error e_y^2

It should be pointed out that the scheme of Figure 6.22 is not the only possible configuration of implementing the system presented. For instance, in order to avoid transmission of both *x* and *y* master signals across the channel, it is possible to introduce a differentiator at the receiver side and pass the received *x* signal through it to obtain an estimate of the master *y* signal, as from equation 5.3.1, section 5.3, it is observed that in fact $\dot{x} = y$. Such a configuration has the advantage from the aspect of the reduced bandwidth requirement by transmitting a single signal instead of two interleaved signals. However, in this case, the robustness to noise of the system is significantly reduced as is demonstrated by the open squares BER curve of Figure 6.24.

Yet another, more robust scheme which shows how to implement the Ueda ICM scheme by transmitting only the master signal *x* is proposed. This scheme is outlined in the appendix [15]. In this particular configuration it is shown that the

transmitted bits can be recovered by only observing the slave signal $\hat{y}$ thus eliminating the requirement of transmitting the master signal y as well.

Similar ICM based communication systems can also be constructed as is demonstrated in the next two subsections on the simplest quadratic and the simplest piecewise linear master-slave chaotic flows.

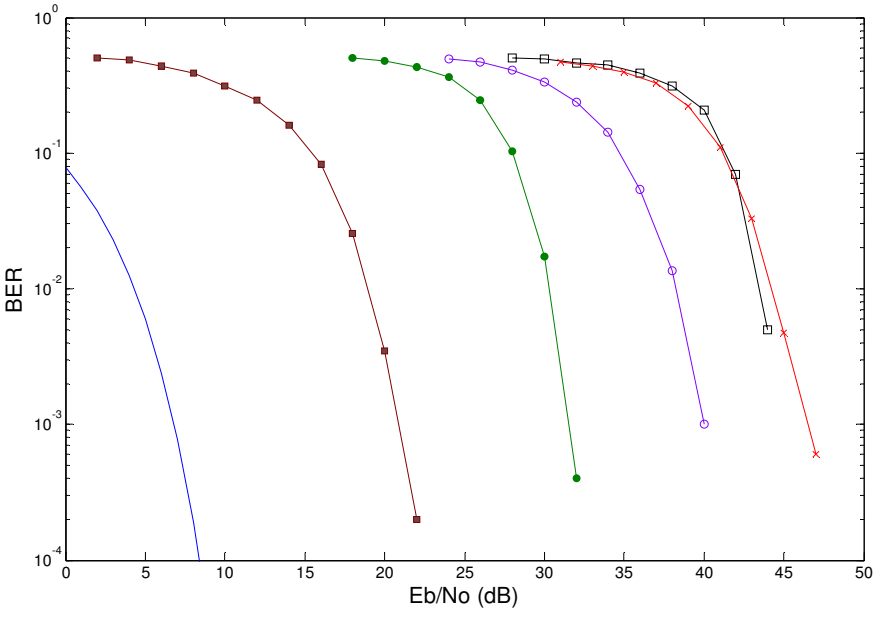

Fig. 6.24 The BER curves: (a) the solid line is for the theoretical BPSK, (b) the solid circles are for the Ueda ICM based system of Figure 6.22, (c) the crosses are for the Lorenz CPM based system of Figure 6.7 [8], (d) the open squares are for the Ueda ICM based system of Figure 6.22 but with the differentiator and only x transmitted, (e) the solid squares are for the simplest quadratic ICM based system of Figure 6.25, (f) the open circles are for the simplest piecewise linear ICM based system of Figure 6.27.

6.3.3 The Communication System Implementing the Simplest Quadratic Master-Slave Chaotic Flow

In Figure 6.25 the communication system implementing the simplest quadratic master-slave chaotic flow is outlined.

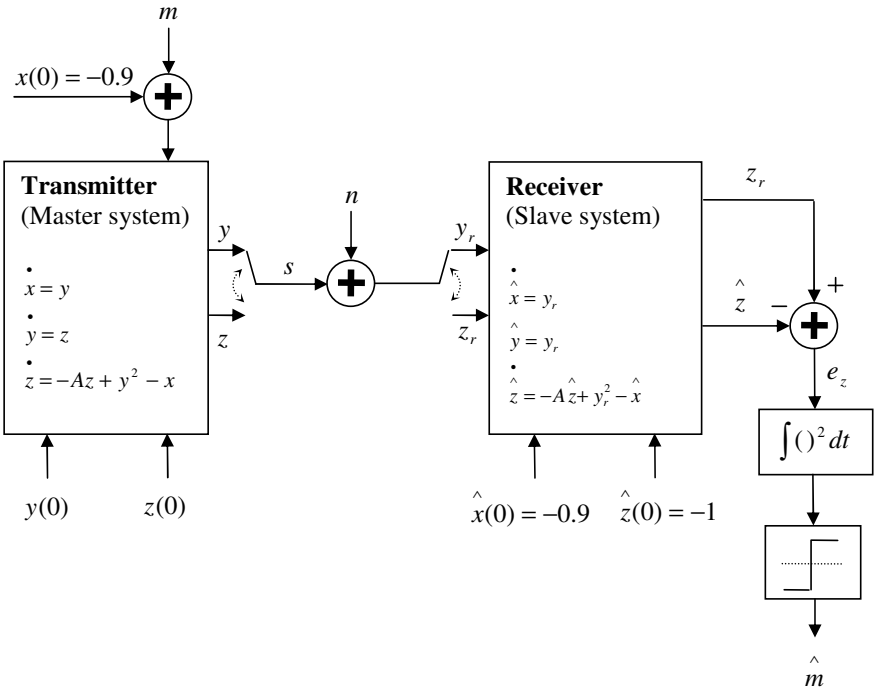

Fig. 6.25 The simplest quadratic chaotic communication system based on the initial condition modulation

The transmitted signal s is a signal composed of y and z master signals, interleaved in the same fashion as signals x and y of the previous section. The signals y_r and z_r, are described by equations 6.3.8 and 6.3.9, respectively:

$$y_r(t) = y(t) + n_y(t) = \sum_{i=1}^{N} (y_t + n_{y\,t})\,\delta(t - 2i + 1) \tag{6.3.8}$$

$$z_r(t) = z(t) + n_z(t) = \sum_{i=1}^{N} (z_t + n_{z\,t})\,\delta(t - 2i) \tag{6.3.9}$$

The operation of the communication system of Figure 6.25 is based on the synchronization error of the master-slave z signals. It has been shown in section 5.2 [10] that after the transients die down, the synchronization error of the master-slave z signals is governed by equation 5.2.22, repeated below as equation 6.3.10 for convenience:

$$\delta = -\frac{\alpha}{A} \tag{6.3.10}$$

Recall that in equation 6.3.10, $\alpha = x(0) - \hat{x}(0) = x - \hat{x}$, and A is the system parameter.

The master initial condition of the x signal is varied according to the value of the bit to be transmitted, bit 1 being represented by $m = 8.9$ and bit 0 by $m = 0$. Such choice of m ensures that the distance of symbols (bits) in their symbol space is large, while still maintaining the chaotic properties of the system. The symbol space of this system is limited by the basin of attraction of the initial conditions of the simplest quadratic chaotic flow and therefore care must be taken in the choice of the initial conditions [22] to avoid the system going off to infinity.

To avoid periodicity of chaotic sequences representing bit 0 (or bit 1), it is essential to alter $y(0)$ and $z(0)$ with every new bit sent. However, in this case, the initial conditions of y and z for every new bit transmitted have not been chosen as the final values of the chaotic carrier of the preceding bit, due to the limited basin of attraction of the initial conditions. Instead, they have been randomly assigned within the basin of attraction for every new bit transmitted. This ensures the chaotic properties of the system; however, it may jeopardize the security of the system as compared to the system of Figure 6.22, due to the non-smooth bit transitions and the more restricted choice of initial conditions. The interleaved transmitted signal s is shown in Figure 6.26 when the series of 10 bits is transmitted, that is, when $m = [2\pi, 2\pi, \pi, 2\pi, \pi, \pi, 2\pi, \pi, 2\pi, \pi]$, or in binary terms: *message* = [0 0 1 0 1 1 0 1 0 1]. Figure 6.26 also shows the corresponding squared synchronization

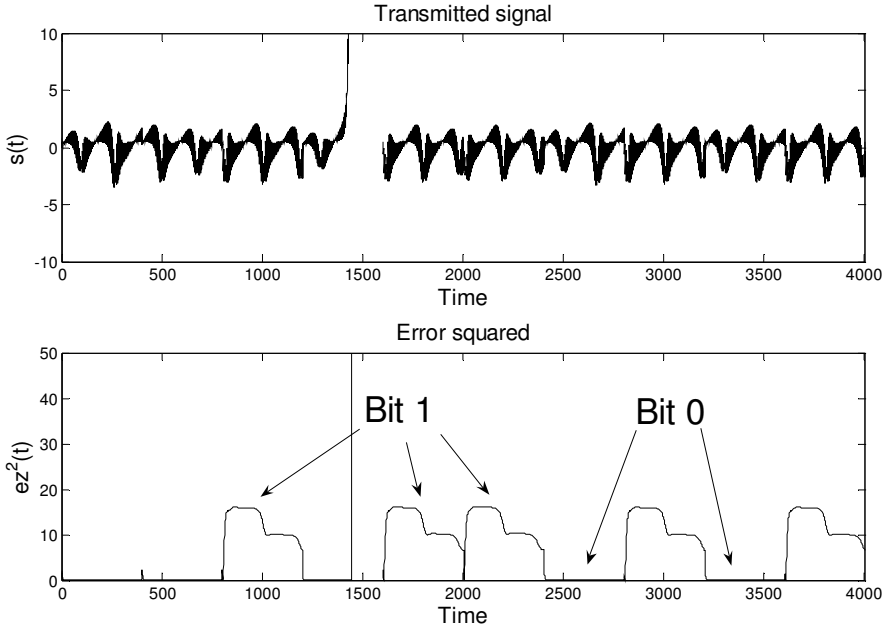

Fig. 6.26 The interleaved transmitted signal s, and the squared synchronization error e_z^2

error, e_y^2, under noiseless conditions. The spreading factor of 400 has been used. From Figure 6.26 one can observe that the transmitted signal diverges to infinity if the chosen initial conditions of a particular bit are not within the basin of attraction.

The result of the BER analysis for the simplest quadratic ICM based system of Figure 6.25 is displayed in Figure 6.24 by the curve marked by solid squares. From Figure 6.24 it is observed that it requires 11-12 dB less energy per bit to achieve the same probability of error using the simplest quadratic ICM based system of Figure 6.25 as compared to the Ueda ICM based system of Figure 6.22.

6.3.4 The Communication System Implementing the Simplest Piecewise Linear Master-Slave Chaotic Flow

In Figure 6.27 the communication system implementing the simplest piecewise linear master-slave chaotic flow, where the transmitted signal *s* is composed of the interleaved signals *y* and *x*, is outlined.

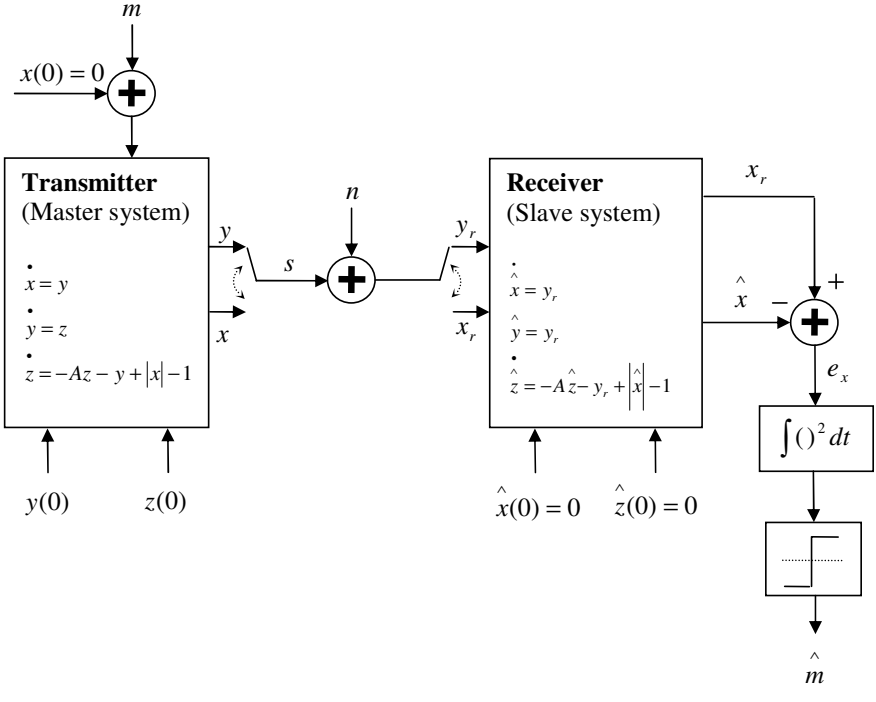

Fig. 6.27 The simplest piecewise linear chaotic communication system based on the initial condition modulation

The signals y_r and x_r, are described by equations 6.3.11 and 6.3.12, respectively:

$$y_r(t) = y(t) + n_y(t) = \sum_{i=1}^{N} (y_t + n_{yt})\,\delta(t - 2i + 1) \tag{6.3.11}$$

$$x_r(t) = x(t) + n_x(t) = \sum_{i=1}^{N} (x_t + n_{xt})\,\delta(t - 2i) \tag{6.3.12}$$

The operation of the communication system of Figure 6.27 is based on the synchronization error of the master-slave x signals, represented by equation 5.1.7, and repeated below as equation 6.3.13 for convenience:

$$x - \hat{x} = x(0) - \hat{x}(0) = J \tag{6.3.13}$$

The initial condition of the master signal x is varied according to the value of the bit to be transmitted, bit 1 being represented by $m = 1$ and bit 0 by $m = 0$. Such a choice of m ensures that the separation of symbols (bits) in their symbol space is relatively large, while still maintaining the chaotic properties of the system, that is, preventing the system from going off to infinity. In order to preserve smoothness of the transmitted chaotic sequence y, as well as to avoid periodicity, the initial condition of y for every new bit transmitted is chosen as the final value of the chaotic carrier of the preceding bit. The disadvantage of this system is that the initial conditions of the master signal x modulate the message to be transmitted while at the same time transmitting the master signal x, thus jeopardizing the security of the information transmitted as compared to the systems of Figure 6.22 and Figure 6.25. The interleaved transmitted signal s is shown in Figure 6.28 when the series of 10 bits is transmitted, that is, when m = [2π, 2π, π, 2π, π, π, 2π, π, 2π, π], or in binary terms: *message* = [0 0 1 0 1 1 0 1 0 1]. Figure 6.28 also shows the corresponding squared synchronization error, e_y^2, under noiseless conditions. The spreading factor of 400 has been used. From Figure 6.28 one can observe that the transmitted signal does not diverge to infinity at any time if the chosen initial conditions of a particular bit are within the basin of attraction.

The result of the BER analysis for the simplest piecewise linear ICM based system of Figure 6.27 is displayed in Figure 6.24 by the curve marked by open circles. From Figure 6.24 it is observed that it requires 6-9 dB more energy per bit to achieve the same probability of error using the simplest piecewise linear ICM based system of Figure 6.27 as compared to the Ueda ICM based system of Figure 6.22.

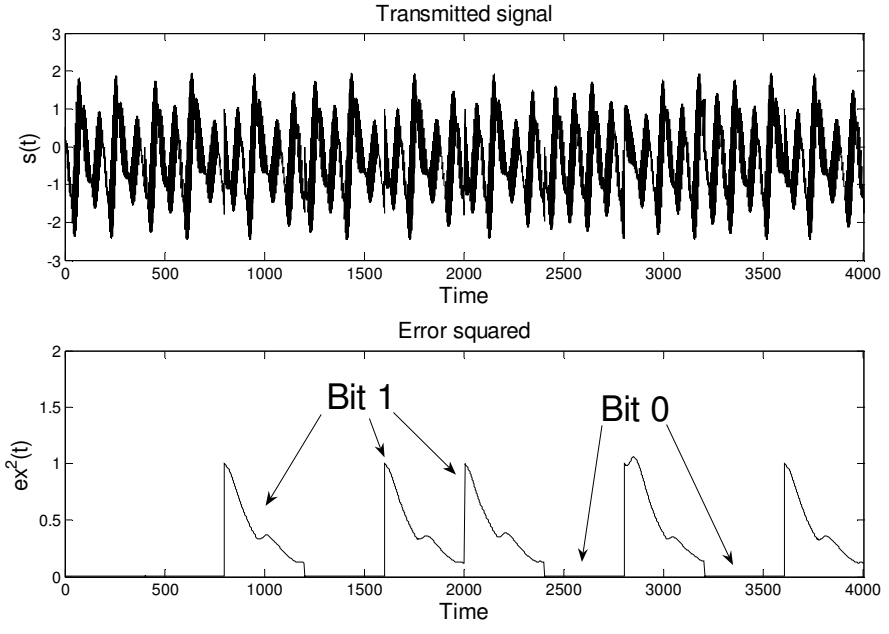

Fig. 6.28 The interleaved transmitted signal *s*, and the squared synchronization error e_x^2

6.3.5 Discussion

In this section the three chaotic communication systems, based on the initial condition modulation of the message to be transmitted, have been presented. They are now discussed in terms of their performance.

The communication system based on the simplest quadratic master-slave chaotic flow exhibits the best performance in terms of the bit error rate, as compared to the other two systems, due to the largest relative separation of the bits transmitted in their symbol space at the receiver. Due to having the smallest relative separation of the bits transmitted in their symbol space, the communication system based on the simplest piecewise linear master-slave chaotic flow exhibits the worst bit error rate performance.

From the security point of view, the communication system based on the Ueda master-slave chaotic system may offer the most security out of the three systems presented, as this system is not limited by the basin of attraction. This allows for the widest range of initial conditions for the message modulation, that is, it enables for the smooth nature of the transmitted signal at the bit transitions. The communication system based on the simplest piecewise linear master-slave chaotic flow uses the error of the master-slave *x* signals to demodulate the message while at the same time the initial conditions of the transmitted master signal *x* modulate the message. This can be seen from equation 6.3.13 and Figure 6.27. Therefore the security of this system is jeopardized as compared to the other two

systems whose demodulation, that is, steady state synchronization error, equations are independent of their own initial conditions, but depend on the modulating initial conditions of the signal not transmitted. This can be seen from equations 6.3.1 and 6.3.10, and Figures 6.22 and 6.25, respectively.

6.4 Performance Evaluation in the Presence of Noise

In this section, the noise performance of the binary modulation techniques of sections 6.2 and 6.3 is examined and compared in terms of the bit error rate.

In Figure 6.29 the BER performance of the Lorenz, Ueda and cubic CPM systems is compared to that of the ICM systems of section 6.3. Furthermore, the BER curve of the filtered and plain Ueda ICM system with only x transmitted [15], (outlined in the appendix), is also presented.

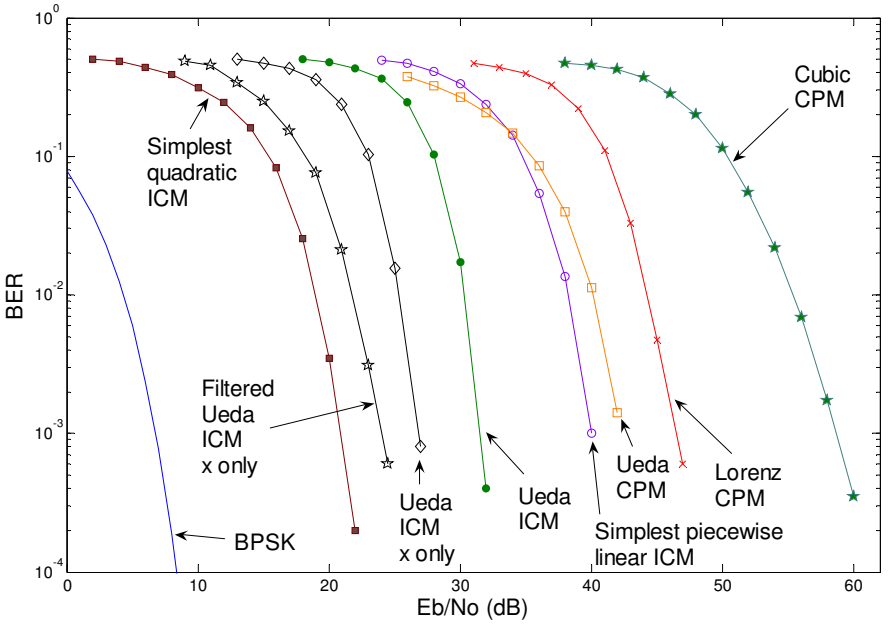

Fig. 6.29 The BER curves: (a) the solid line is for the theoretical BPSK, (b) the solid squares are for the simplest quadratic ICM system of Figure 6.25 [10], (c) the open pentagram stars are for the Filtered Ueda ICM system of the appendix [15], (d) the open diamonds are for the Ueda ICM system of the appendix [15], (e) the solid circles are for the Ueda ICM system of Figure 6.22 [10], (f) the open circles are for the simplest piecewise linear ICM system of Figure 6.27 [10], (g) the open squares are for the Ueda CPM system of Figure 6.14 [16], (h) the crosses are for the Lorenz CPM system of Figure 6.7 [8], (i) the open pentagram stars are for the cubic CPM system of Figure 6.17.

While evaluating the BER curves of Figure 6.29 it has been assumed that the clock synchronization among the clock at the transmitter and the clock at the receiver has already been achieved. As discussed in chapter 1, this assumption is used in most cases when evaluating the performance of binary modulation techniques [20,10].

From Figure 6.29 it is observed that it requires 7-10 dB less energy per bit to achieve the same probability of error using the Ueda ICM system as compared to the Ueda CPM system. Furthermore, it requires 4-6 dB less energy per bit to achieve the same probability of error using the Ueda CPM system as compared to the Lorenz CPM system. Therefore, the Ueda ICM system exhibits better noise performance than the Ueda CPM system which in turn exhibits better noise performance than the Lorenz CPM system. However, most importantly, it should be observed that all of the ICM based systems developed here outperform the CPM based systems. In particular, the best performance is exhibited by the simplest quadratic ICM based system and the worst by the cubic CPM based system. Although the simplest quadratic ICM based chaotic communication system exhibits the best performance in terms of BER it has been argued in section 6.3 that it may not be the most secure system. Similarly, it was argued that Ueda ICM based system exhibits the best overall performance in terms of security and BER. Therefore, the further 4-5 dB BER improvement exhibited by the Ueda ICM based system with only the master signal x transmitted over the Ueda ICM based system with both master x and y signals transmitted (Figure 6.22) is of particular importance. Furthermore, it has been shown in the appendix [15] that by applying filters to the received signal x further improves the performance of the system by 3-4 dB. However, it can be observed from Figure 6.29 that even the simplest quadratic ICM based system which exhibits the best BER performance, out of all of the chaotic synchronization based systems examined, is still outperformed by the BPSK system by approximately 14 dB. In the next chapter, a robust synchronization unit for the chaos based DS-CDMA systems is proposed. It is shown that in terms of BER it outperforms the communication systems based on the principle of chaotic synchronization presented and examined in this chapter.

It should be noted that all of the communication systems presented in this chapter are inherently single user systems. It will be shown in chapter 9, how principles of TDM can be used to allow these systems to become multi-user systems. Their performance will be examined in both AWGN and Rayleigh fading channels. Furthermore, it will be shown that by using different receiver architectures BER performance can be improved in certain cases.

6.5 Conclusion

In this chapter, several chaotic communication systems with the receiver based on chaotic synchronization have been described. These include the chaotic communication schemes of chaotic masking, chaotic modulation and the new chaotic communication scheme of initial condition modulation.

It has been shown how Lyapunov's direct method presented in chapter 3 can be used in the design of CPM based communication systems. In particular, this has been shown on the Ueda master-slave chaotic system.

Furthermore, a method of implementing the synchronized chaotic map master-slave system of chapter 4 within a CPM based secure communication system, was demonstrated on the $\Re^1$ cubic map. It was shown that instant synchronization within the chaotic map CPM based communication system allows for the highest level of discrimination among bits 0 and 1.

On the basis of findings of chapter 5, a secure communication system based on the initial condition modulation of the chaotic carrier by the binary message was then presented. In particular, this system utilizes a novel approach to the master-slave synchronization properties of the three chaotic flows investigated. The empirical BER curves for the presented communication systems have then been produced and compared to the empirical BER curve of the Lorenz CPM based communication system of [8], demonstrating a significant improvement. It has been shown that the communication system based on the simplest quadratic master-slave chaotic flow exhibits the best performance in terms of BER, as compared to the other two presented systems based on the Ueda and the simplest piecewise linear master-slave chaotic flows. From the security point of view it has been observed that the communication system based on the Ueda master-slave chaotic system may be the most secure of the three systems presented.

Finally, the overall performance of the chaotic parameter and initial condition modulation techniques has been examined and compared in the presence of AWGN. It has been shown in terms of BER that the ICM based chaotic communication systems exhibit better noise performance than the CPM based ones. Therefore, most importantly, it can be concluded that all of the chaotic synchronization ICM based systems presented here outperform the presented CPM based systems. Furthermore, it has been shown on the Ueda ICM based chaotic communication system that the denoising techniques can be used to further improve the BER performance. The details of the denoising techniques developed have been described in the appendix. The work of this chapter has been published in [10,16,15].

References

[1] Murali, K., Lakshmanan, M.: Transmission of signals by synchronization in a chaotic Van der Pol-Duffing oscillator. Physical Review E, Rapid Communications 48(3), R1624–R1626 (1993)

[2] Wu, C.W., Chua, L.O.: A unified framework for synchronization and control of dynamical systems. International Journal of Bifurcation and Chaos 4(4), 979–998 (1994)

[3] John, J.K., Amritkar, R.E.: Synchronization of unstable orbits using adaptive control. Physical Review E 49(6), 4843–4848 (1994)

[4] Oppenheim, A.V., Wornell, G.W., Isabelle, S.H., Cuomo, K.M.: Signal processing in the context of chaotic signals. In: Proceedings IEEE ICASSP, pp. 117–120 (1992)

[5] Kocarev, L., Halle, K.S., Eckert, K., Chua, L.O., Parlitz, U.: Experimental demonstration of secure communications via chaotic synchronization. International Journal of Bifurcation and Chaos 2(3), 709–713 (1992)
[6] Parlitz, U., Chua, L.O., Kocarev, L., Hale, K.S., Shang, A.: Transmission of digital signals by chaotic synchronization. International Journal of Bifurcation and Chaos 2(4), 973–977 (1992)
[7] Kapitaniak, T., Sekieta, M., Ogorzalek, M.: Monotone synchronization of chaos. International Journal of Bifurcation and Chaos 6(1), 211–217 (1996)
[8] Cuomo, K.M., Oppenheim, A.V.: Circuit Implementation of Synchronized Chaos with Applications to Communications. Physical Review Letters 71(1), 65–68 (1993)
[9] Cuomo, K.M., Oppenheim, A.V., Strogatz, S.H.: Synchronization of Lorenz-Based Chaotic Circuits with Applications to Communications. IEEE Transactions on Circuits and Systems – II. Analog and Digital Signal Processing 40(10), 626–633 (1993)
[10] Jovic, B., Berber, S., Unsworth, C.P.: A novel mathematical analysis for predicting master – slave synchronization for the simplest quadratic chaotic flow and Ueda chaotic system with application to communications. Physica D 213(1), 31–50 (2006)
[11] Wu, C.W., Chua, L.O.: A simple way to synchronize chaotic systems with applications to secure communication systems. International Journal of Bifurcation and Chaos 3(6), 1619–1627 (1993)
[12] Halle, K.S., Wu, C.W., Itoh, M., Chua, L.O.: Spread spectrum communication through modulation of chaos. International Journal of Bifurcation and Chaos 3(2), 469–477 (1993)
[13] Lu, J., Wu, X., Lü, J.: Synchronization of a unified chaotic system and the application in secure communication. Physics Letters A 305(6), 365–370 (2002)
[14] Pecora, L.M., Carroll, T.L.: Synchronization in chaotic systems. Physical Review Letters 64(8), 821–824 (1990)
[15] Jovic, B., Unsworth, C.P., Berber, S.M.: De-noising 'Initial Condition Modulation' Wideband Chaotic Communication Systems with Linear & Wavelet Filters. In: Proceedings of the First IEEE International Conference on Wireless Broadband and Ultra Wideband Communications (AusWireless 2006), Sydney, Australia, March 13-16, pp. 1–6 (2006)
[16] Jovic, B., Unsworth, C.P.: Synchronization of Chaotic Communication Systems. In: Wang, C.W. (ed.) Nonlinear Phenomena Research Perspectives, Nova Publishers, New York (2007)
[17] Lau, F.C.M., Tse, C.K.: Chaos-Based Digital Communication Systems, ch. 1, pp. 1–20. Springer, Berlin (2004)
[18] Ueda, Y.: Survey of Regular and Chaotic Phenomena in the Forced Duffing Oscillator. Chaos, Solitons and Fractals 1(3), 199–231 (1991)
[19] Kennedy, M.P., Kolumban, G.: Digital Communications Using Chaos. In: Chen, G. (ed.) Controlling Chaos and Bifurcations in Engineering Systems, pp. 477–500. CRC Press LLC, Boca Raton (1999)
[20] Carroll, T.L., Pecora, L.M.: Using multiple attractor chaotic systems for communication. Chaos 9(2), 445–451 (1999)
[21] Reddell, N.F., Welch, T.B., Bollt, E.M.: A covert communication system using an optimized wideband chaotic carrier. In: MILCOM Proceedings, vol. 2, pp. 1330–1334 (2002)
[22] Sprott, J.C.: Chaos and Time-Series Analysis, pp. 230–440. Oxford University Press, Oxford (2003)